RSMC Tokyo – Typhoon Center

Technical Review

No. 3

Contents

Japan Meteorological Agency

March 1999

Suppressed Tropical Cyclone Formation in 1998

Tetsuo Nakazawa
Typhoon Research Department, Meteorological Research Institute,
Japan Meteorological Agency

Abstract

Tropical cyclone formation was markedly suppressed in the northwestern Pacific during 1998. To explore this, we contrast monthly mean fields for January, March, May, and July 1998 with climatologies, and with what is known about the preferred regions and mechanisms for tropical cyclogenesis by season. The atmospheric variables of interest include, surface wind speed, rainfall, outgoing longwave radiation, total precipitable water, sea surface temperature (SST), and upper level velocity potential. Prior to June 1998, the El Niño/Southern Oscillation (ENSO) warm event of 1997-98 dominated the atmospheric circulation in the tropical Indian and Pacific Ocean basins. A rising motion anomaly was evident just south of the equator in the eastern Pacific. Consistent with this anomaly were increased convective activity, wetter than normal air, and higher than normal SST. A center of anomalous subsidence was located over the western Pacific for the same time period. Consistent with that anomaly were suppressed convective activity, and drier than normal air. The rising and subsiding anomaly pair defines a shift in the local Walker circulation that is a signature of an ENSO warm event. This paper argues that suppressed tropical cyclone formation is another effect of this signature.

By July 1998 the ENSO warm event had terminated and the center of rising motion had shifted westward to the Bay of Bengal in contrast to the climatological position in the western Pacific, east of the Philippines. This resulted in a region in the southeastern Indian Ocean of anomalous rising motion, increased convective activity, wetter than normal air, and higher SST.

Compensating anomalous subsidence was again located over the western Pacific in a region that is normally favorable for tropical cyclogenesis. Thus, even though the effects of the ENSO warm event had abated, and even though SST in the western Pacific were anomalously high, the anomalies in the vertical motion of the large-scale circulation were sufficient to suppress tropical cyclone formation.

1. Introduction and Data

In 1998, only 16 tropical cyclones were generated in the northwestern Pacific Ocean region whereas climatological numbers for this region are between 27 and 28. Figure 1 compares the number of tropical cyclone generations by month for all of 1998 with climatology. It was not until 9 July 1998 that the first tropical storm was declared in the western Pacific. This marks the latest date for the first declaration of tropical storm in any year in the records of the Japan Meteorological

Agency (JMA). In a typical boreal summer season (June through August), more than 10 tropical cyclones with tropical storm intensity or higher are generated. In 1998 only four tropical cyclones were declared during summer. A return to normal tropical cyclone generation numbers began to occur in September. However tropical cyclone generation was half the climatological value for October. The numbers matched or exceeded climatology in November and December.

The purpose of this paper is to examine monthly averages of relevant atmospheric fields in light of the abnormal suppression of tropical cyclone generation in 1998. We will examine tropical Indian and Pacific Ocean fields for surface wind speed, rainfall, outgoing longwave radiation (OLR), total precipitable water (TPW), sea-surface temperature (SST), and upper-level velocity potential.

Sources for these data are as follows. Monthly mean rainfall, surface wind speed, and TPW are obtained from the Special Sensor Microwave Imager (SSM/I) data according to the Wentz algorithm (Wentz, 1995; 1996). Monthly mean OLR is taken from the polar orbiting NOAA-12 and 14 dataset. Monthly mean SST is compiled by JMA, and monthly mean upper-level velocity potential is provided in the NOAA National Centers for Environmental Prediction (NCEP) global objective analyses.

2. Tropical Cyclogenesis

Gray (1979) argues that six parameters are sufficient to determine climatological tropical cyclone generation. These parameters are: SST, relative vorticity in the lower troposphere, the local planetary vorticity (e.g. Coriolis parameter), vertical wind shear, vertical stability and relative humidity in the middle troposphere. Palmén (1948) noted that tropical cyclones do not form when

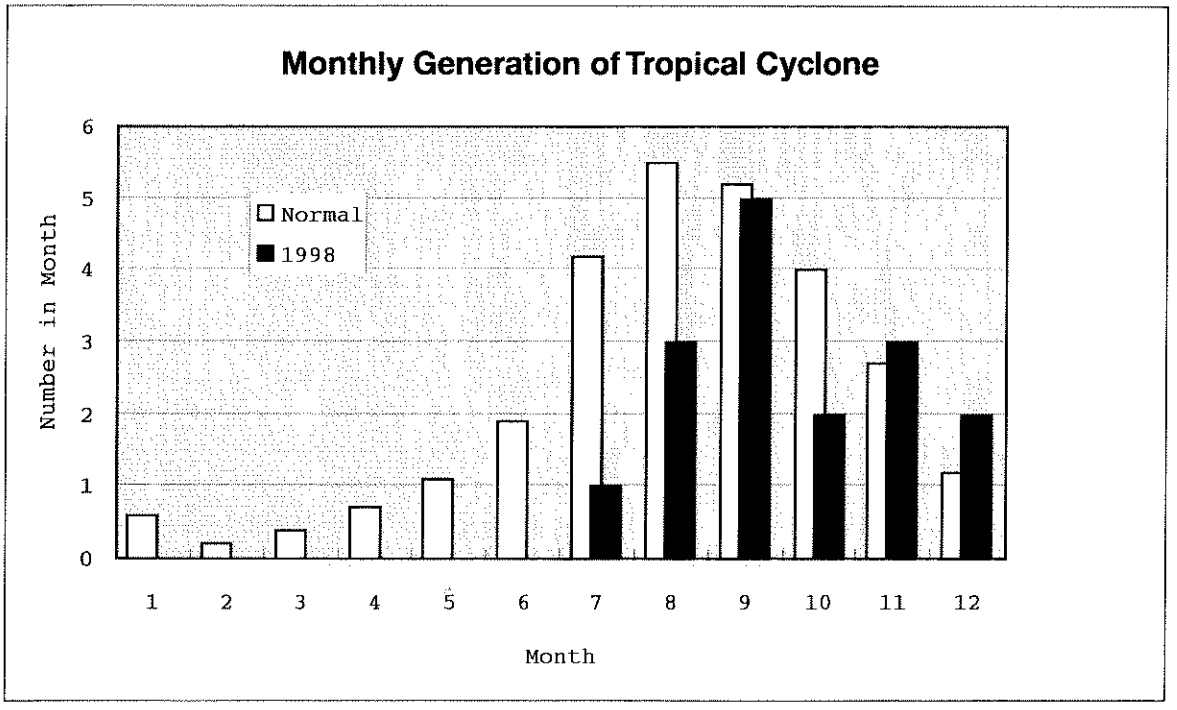

Figure 1 Monthly generation number of tropical cyclone with tropical storm intensity or higher for the northwestern Pacific in 1998 (■) and in a climatology from 1961-1990(□)

SST dips below a threshold value of 26 - 27 °C. Nakazawa (1986) showed that tropical cyclone generation tends to occur when 30-60 day intraseasonal variability (e.g. the Madden-Julian oscillation) peaks in the Indian or Pacific Ocean basins. Takayabu and Nitta (1993) analyzed the fine structure of the intraseasonal oscillation and showed that the associated tropical cyclone generation patterns are of two types; a tropical depression type occurring over the tropical northwestern Pacific, and a mixed Rossby-gravity wave type that occurs in the central Pacific near the dateline.

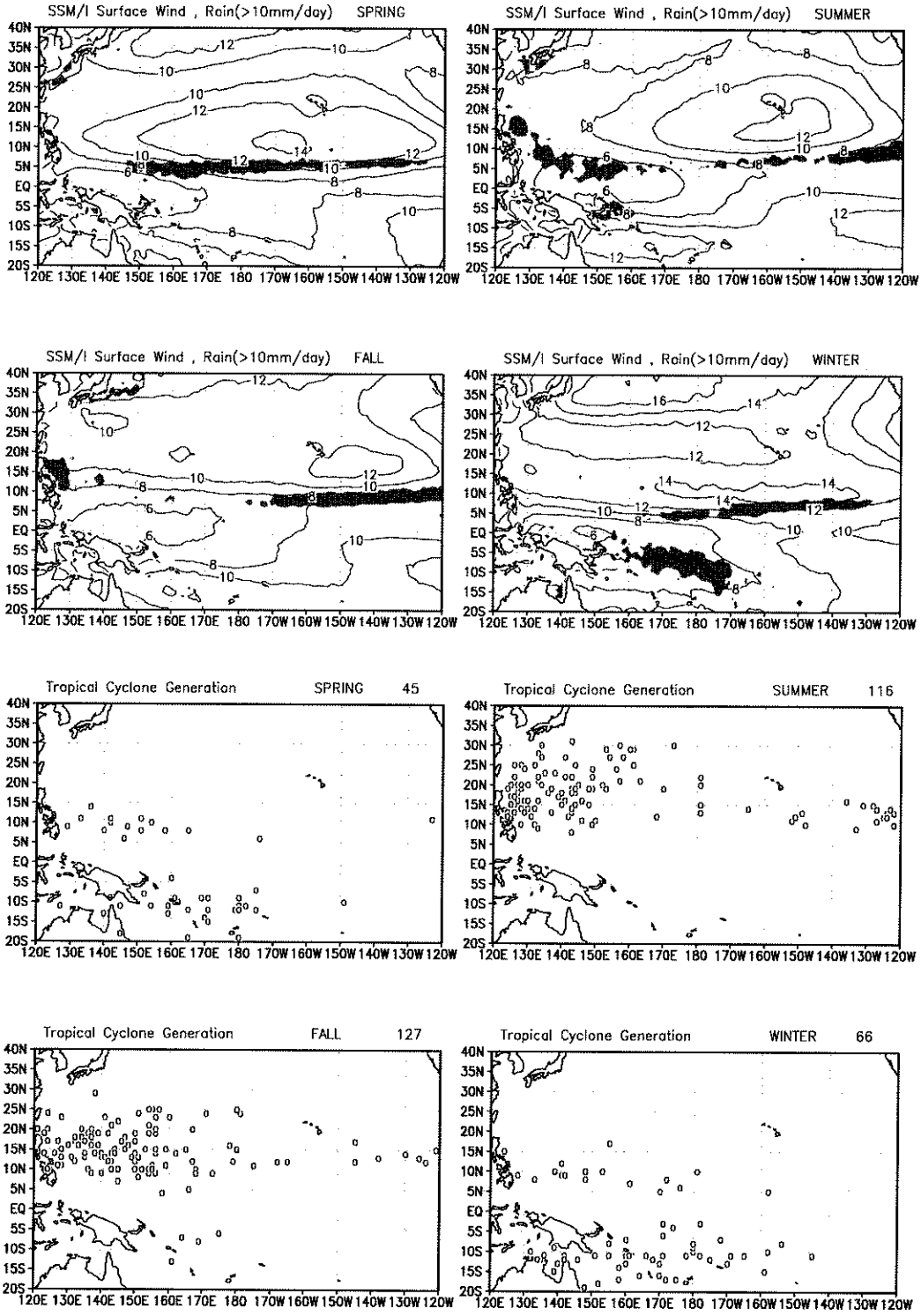

Figure 2 Upper 4 panels: Seasonal mean surface wind speed and rainfall rate greater than 10 mm/day obtained from the 10-year SSM/I Wentz dataset for the 1987-1996 period. Lower 4 panels: Positions of tropical cyclone generations by season during the same 10 year period as in the upper figure.

There are several studies documenting that tropical cyclone formation is suppressed during El Niño/Southern Oscillation (ENSO) warm events (Aoki, 1985, Li, 1988, Wu and N.-C. Lau, 1992).

While the generation mechanism for individual tropical cyclones might not be known precisely, it is generally accepted that generation mechanisms occur in two broad classes. In what we call the coupling-type, tropical cyclogenesis occurs when an upper-tropospheric cold low pressure system and a cloud cluster in the intertropical convergence zone (ITCZ) coincide. A second mechanistic class for tropical cyclogenesis depends on lower-tropospheric wind shear. The origin and early stages of tropical cyclogenesis can be traced readily for the coupling-type mechanism. Development from tropical depression to tropical storm occurs rapidly in the lower tropospheric wind shear mechanistic class. A climatology for the occurrence of tropical cyclogenesis by class can be described from Figures 2a and b. Figure 2a (upper four panels) shows the SSM/I seasonal wind speed (contour) and rainfall rate greater than 10 mm/day (shading) from the 10-year (1987-1996) data set due to Wentz (1995, 1996).

Figure 2b (lower four panels) also depicts the locations of tropical cyclone formations for the same time period. The total number of cyclones in the 10-year period is noted for each season in the upper right of corners for each panel in Figure 2b. In the summer/winter seasons (right hand columns in Figures 2a and b), the rainfall maxima center on the weakest wind speed regions in the summer hemispheres. Tropical cyclone formations for June-August (Figure 2b, upper right) occur poleward of the maximum rainfall region, and concentrate in the lowest wind speed region of the western Pacific (i.e. just east of the Philippines). Analogous patterns occur for Southern Hemisphere summer (lower right hand panels Figures 2a and b), where tropical cyclone formations concentrate just east of Australia and New Guinea. These patterns are consistent with coupling-type cyclogenesis in the summer hemispheres since wind speeds are low, and meridional gradients in wind speed are flat (i.e. no wind shear).

Conversely, during equinox seasons (left hand columns in Figures 2a and b), the rainfall maxima locate over regions of strong meridional gradients in wind speed (also true for the winter hemisphere during December through February). This implies that tropical cyclone formations during spring and fall are associated predominantly with the lower troposphere wind shear-type mechanism.

3. Monthly Mean Fields

In this section we examine monthly mean fields for 1998 for the variables listed in the introduction. We compare these fields with climatologies for the same months to detect anomaly patterns that might explain the extraordinary suppression of tropical cyclone generation in 1998. The same four monthly mean fields (January, March, May and July) are depicted for each variable. For each monthly mean, there are three panels. The top panel is the monthly mean field for the given month in 1998, the middle panel is the climatology for the given month, and the bottom panel is the 1998 anomaly computed by subtracting the middle panel from the top panel for each month.

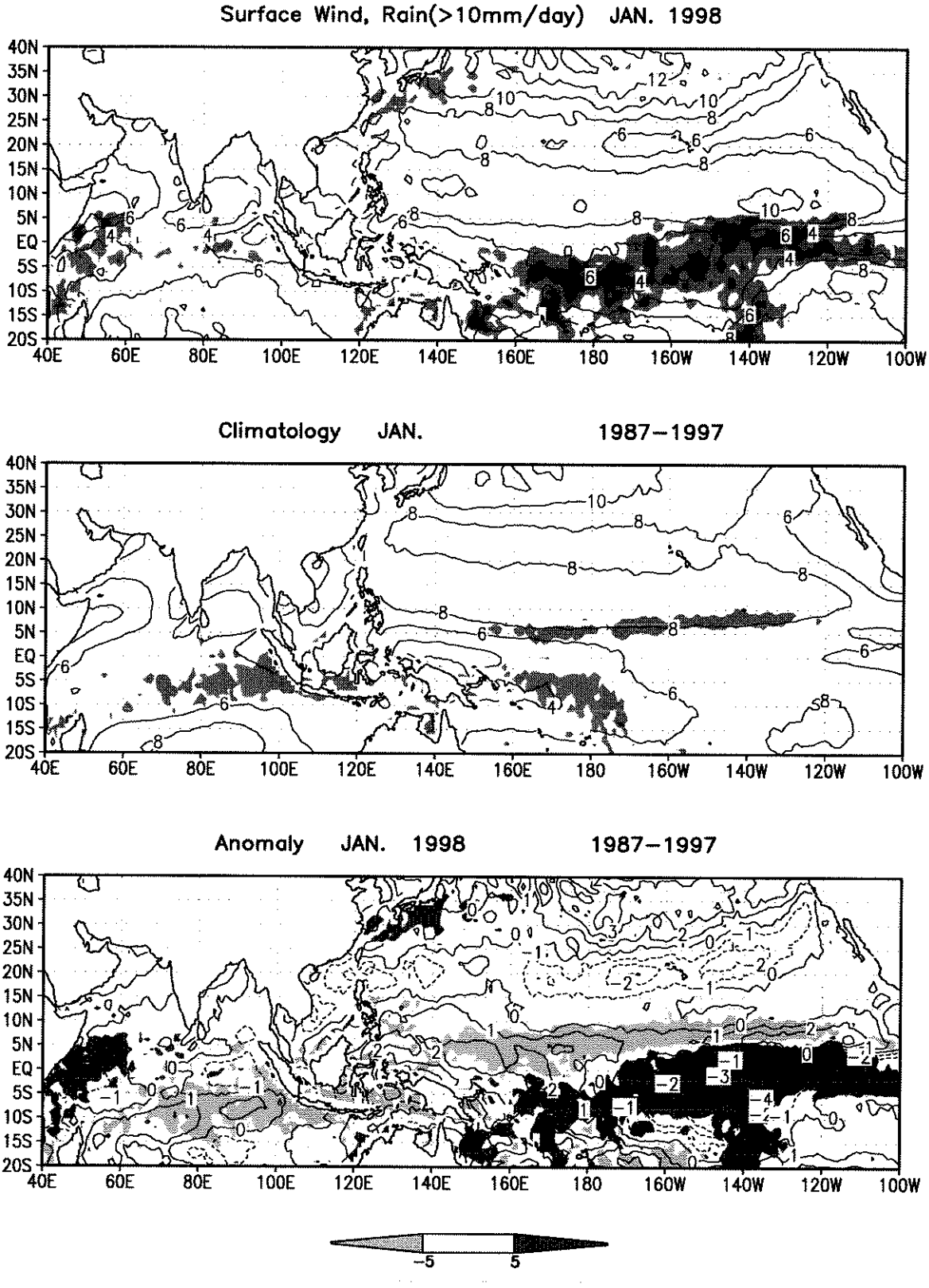

Figure 3a Monthly mean surface wind speed (contour) and rainfall rate(shading). Top: In January 1998. Heavy(light) shading denotes the rainfall rate greater than 20 (10) mm/day. Contour inteval is 2 m/s. Middle: Climatology. Shading is the same as in the top figure. Bottom: Anomaly in January 1998. Heavy(light) shading denotes the rainfall rate anomaly greater than 5 (-5) mm/day. Contour interval is 1 m/s.

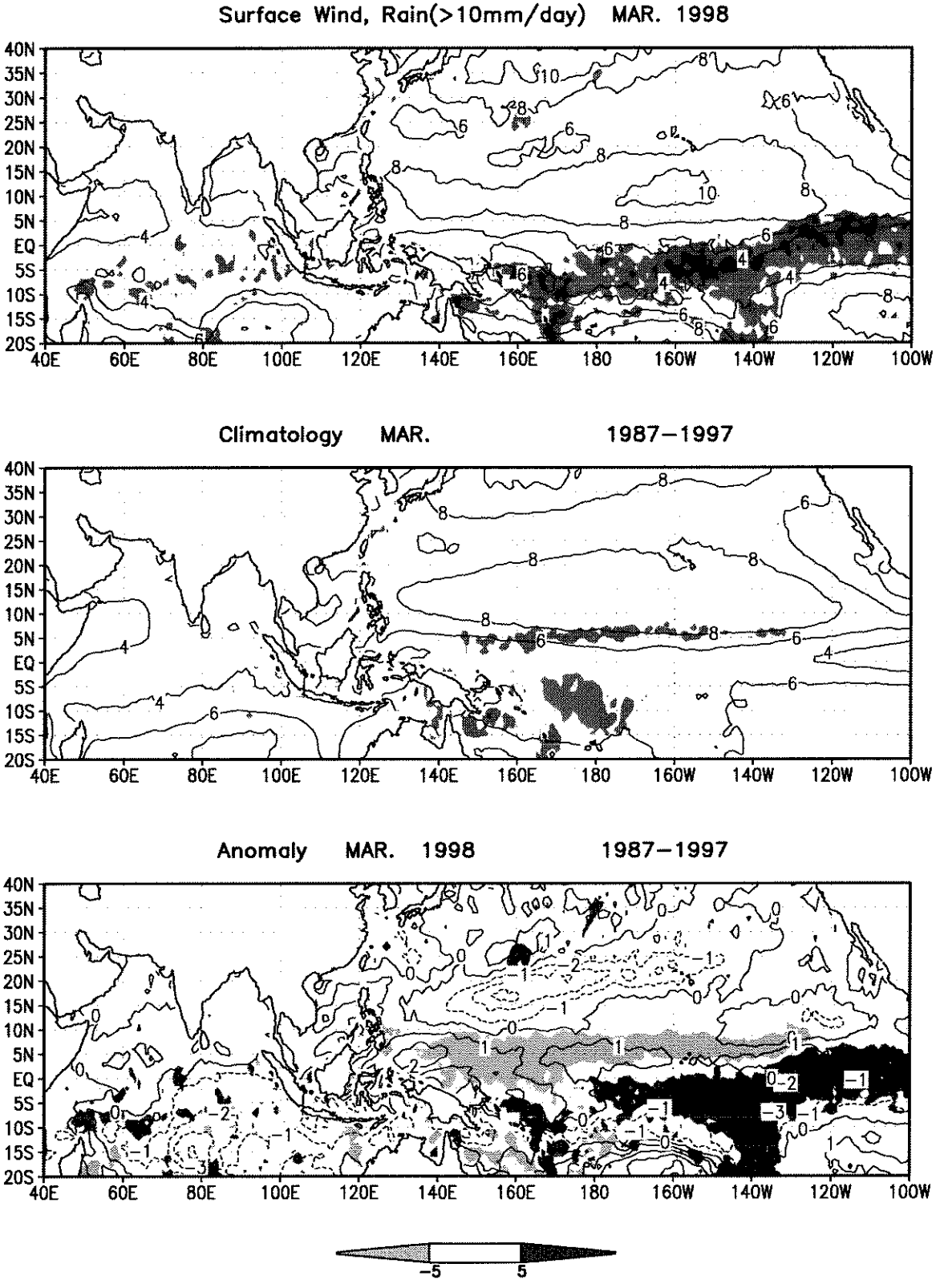

Figure 3b Same as Fig. 3a but for in March 1998.

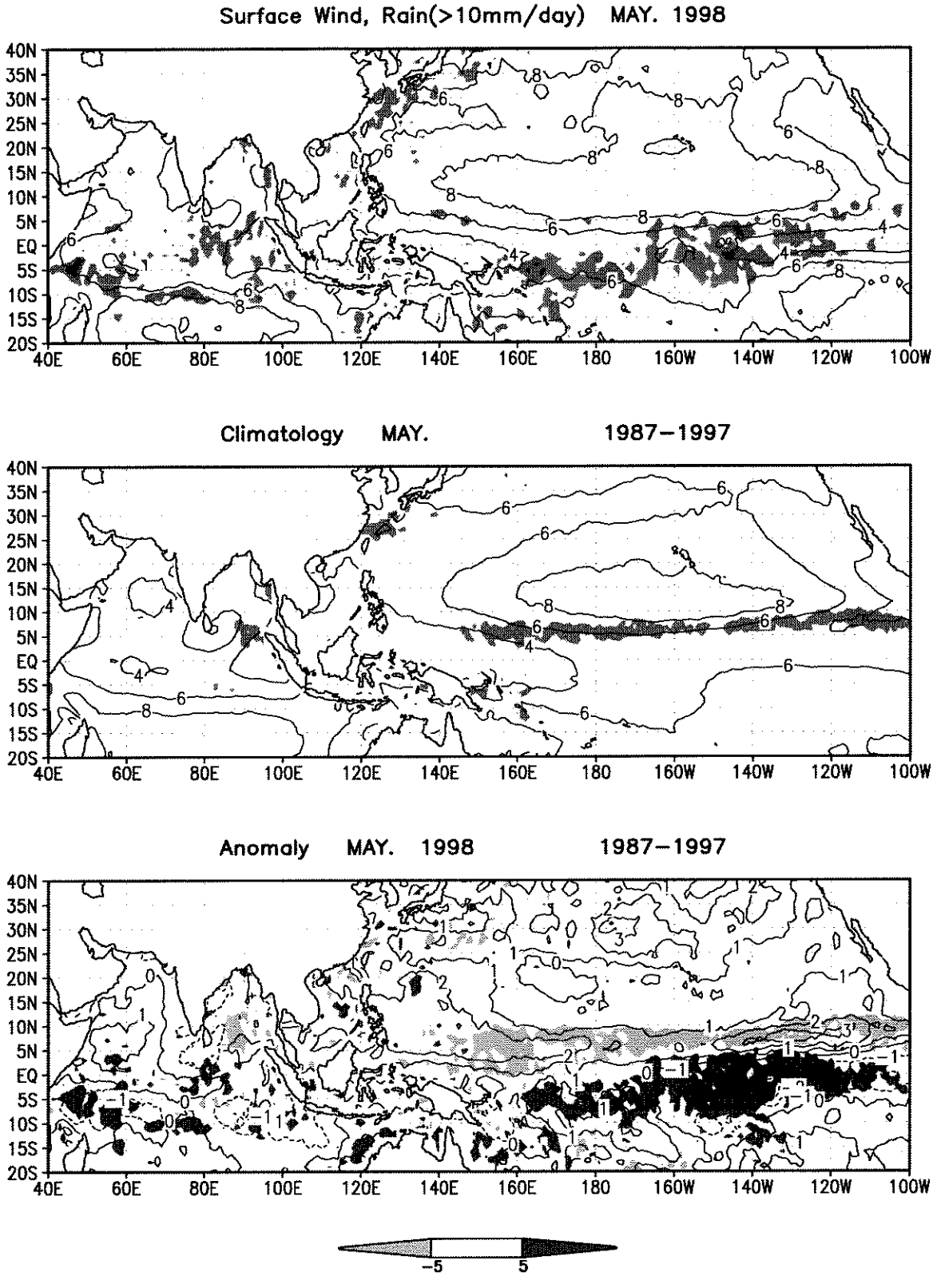

Figure 3c Same as Fig. 3a but for in May 1998.

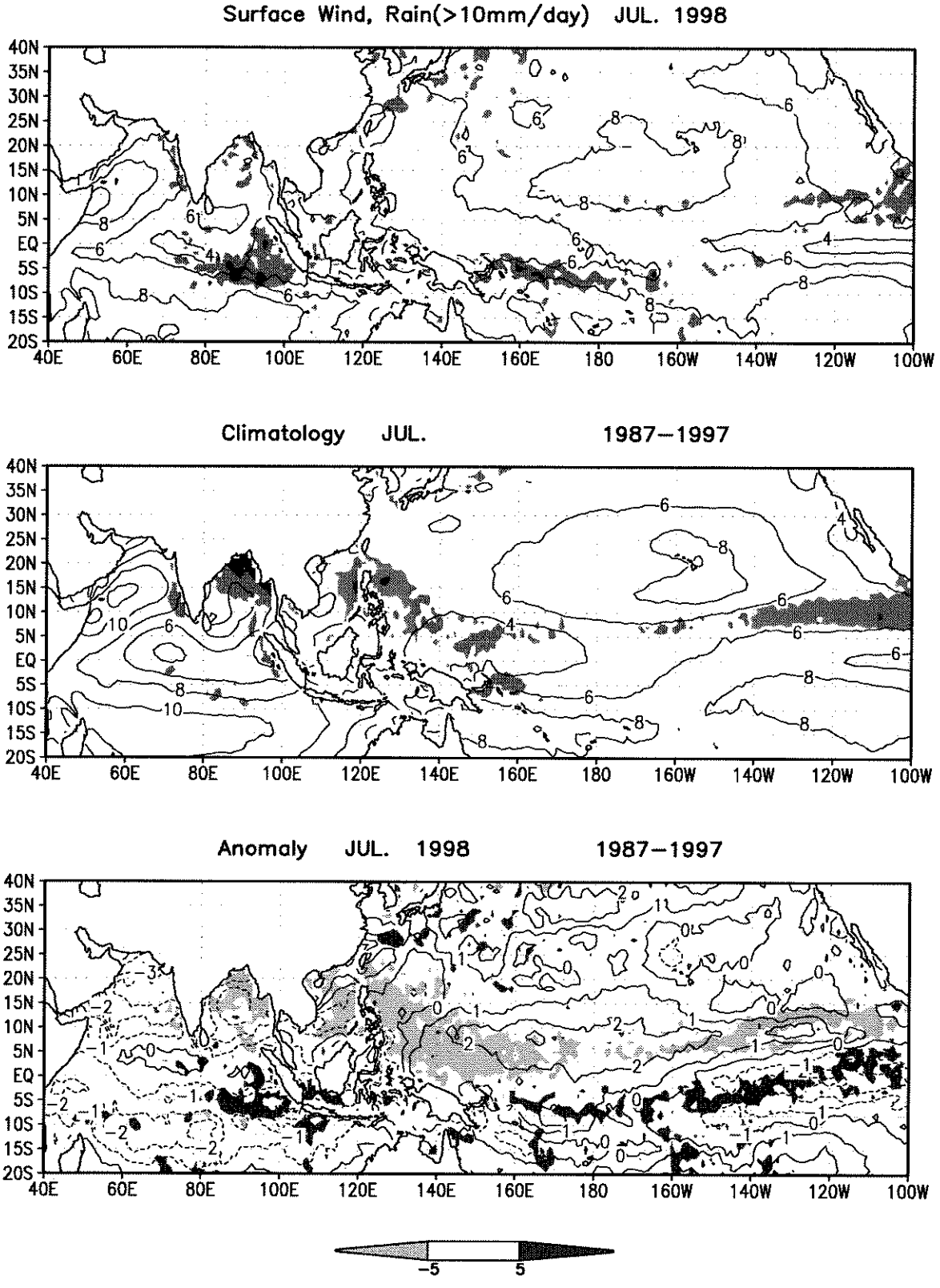

Figure 3d Same as Fig. 3a but for in July 1998.

3a. Rainfall and Surface Wind Speed

Figures 3a shows monthly mean surface wind speed (contours) and rainfall (shading) for January 1998 with climatological January based on the period 1987-1997. In January 1998 (top panel), extreme rainfall amounts occur in a broad band (with large regions of greater than 20 mm/day indicated by heavy shading) that extends east-northeastward from 5 °S 170 °E to the equator at 140 °W, and eastward along the equator to 100 °W. These heavy rains are associated with the mature phase of the 1997-98 ENSO warm event.

This contrasts with the January climatology (middle) where heavy rains are indicated along a narrow east-west line between 5 °N and 10 °N, from 160 °E to 120 °W, representing the climatological ITCZ. There is no rainfall signature consistent with an ITCZ in January 1998 (top). The January 1998 mean rainfall differs from climatology in the Indian Ocean as well. In the climatology (middle), heavy rains occur west of Sumatra (5 °S, 100 °E) to the central Indian Ocean (5 °S, 70 °E).

Instead, in January 1998 the heavy rain area shifted to the western Indian Ocean off the African continent. This rainfall shift is associated with floods in eastern Africa, and drought, high winds, and fires in Indonesia. The January anomaly map (Fig 3a bottom) demonstrates clearly the Pacific and Indian Ocean differences just described. Heavy shading in this panel denotes regions where the rainfall anomaly exceeds or is equal to 5 mm/day, light shading represents regions where the rainfall anomaly is deficit by 5 mm/day or more. Regions of net negative anomaly rainfall associate with regions of positive anomaly wind speeds on the order of 1 m/s. The increased wind speed, reduced rainfall anomaly band stretches from 5 °N 140 °E to 10 °N 120 °W in the Pacific, and from 10 °S 70 °E to Sumatra in the Indian Ocean (i.e. corresponding to the climatological rainfall maxima). Larger amplitude negative wind speed anomalies coincide with regions of anomalously large rainfall amounts. The low wind speed anomalies are as large as -3 and -4 m/s just south of the equator in the eastern Pacific.

Large negative wind speed anomalies are consistent with weakened easterlies associated with the ENSO warm event. The Northern Hemisphere counterparts for negative wind speed anomalies occur in mid-latitudes (20-30 °N) and are not associated with rainfall anomalies there. This is a region of climatological anticyclonic flow associated with quasi-stationary sub-tropical Pacific high pressure systems. The anomaly wind speeds are greater both poleward and equatorward of the region of the sub-tropical high; with the largest anomalies on the poleward side. Increases in wind speeds on the flank of the sub-tropical high are consistent with a strengthening of this pressure system in January 1998. Subsequent fields will indicate that the additional subsidence required to increase the surface high pressure are supplied by the anomalous upward motion that is implied by the rainfall anomaly just south of the equator in the eastern Pacific.

Figures 3b and 3c demonstrate that the January pattern persists in location, but weakens in amplitude through March (Fig. 3b) and May (Fig. 3c). This weakening coincides with the decline of the ENSO warm event which diminished completely by June 1998. Thus the surface wind and rainfall fields for July 1998 (Figure 3d) are markedly different from the preceding months.

The heaviest rainfall that occurred south of the equator in the eastern Pacific has abated,

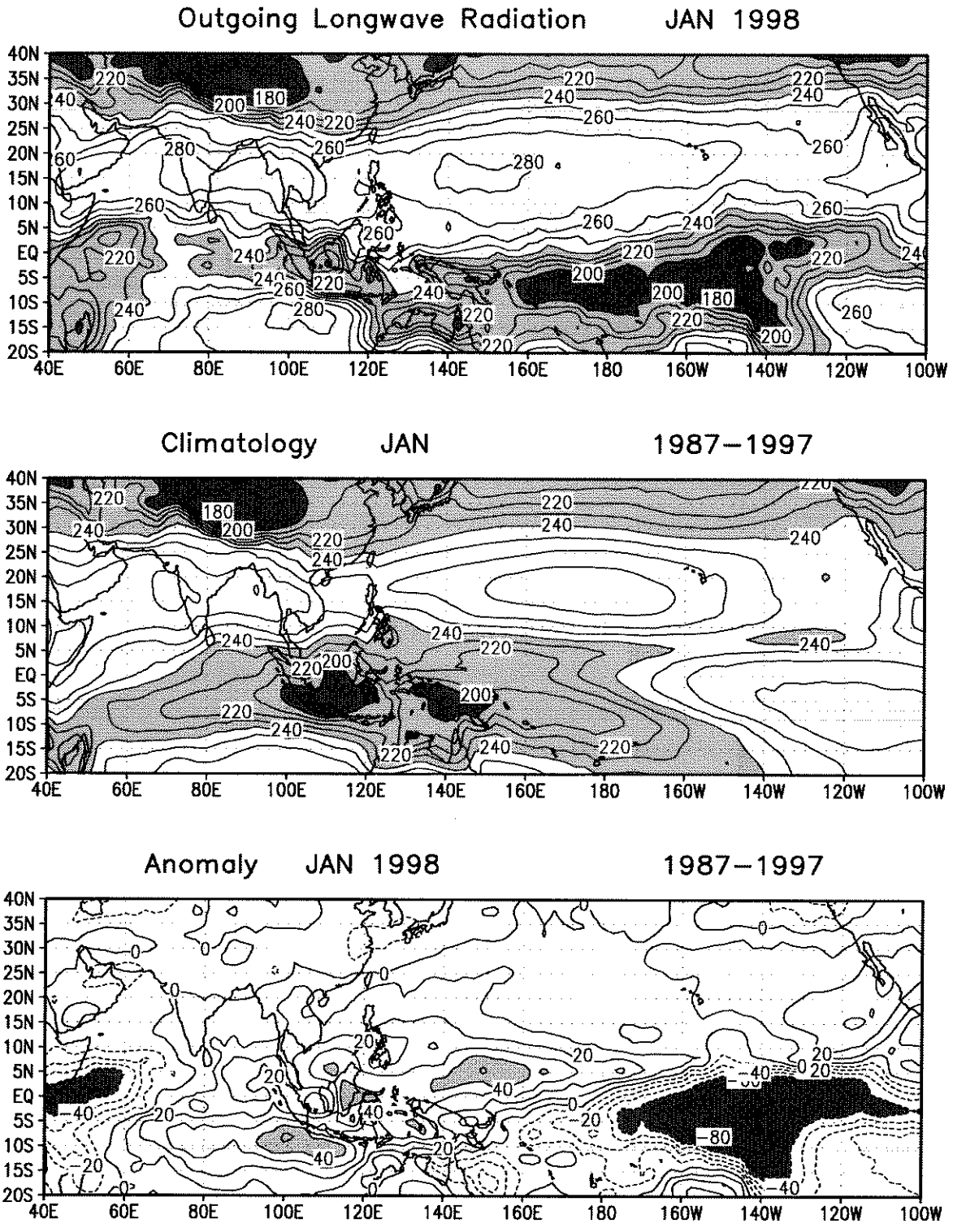

Figure 4a Same as in Fig. 3a but for the outgoing longwave radiation. Top: In January 1998. Heavy(light) shading denotes the region less than 200 (240) Wm^{-2}. Middle: Climatology. Shading is the same as in the top figure. Bottom: Anomaly in January 1998. Heavy shading denotes the region less than -40 Wm^{-2}, light shading greater than +40 Wm^{-2}.

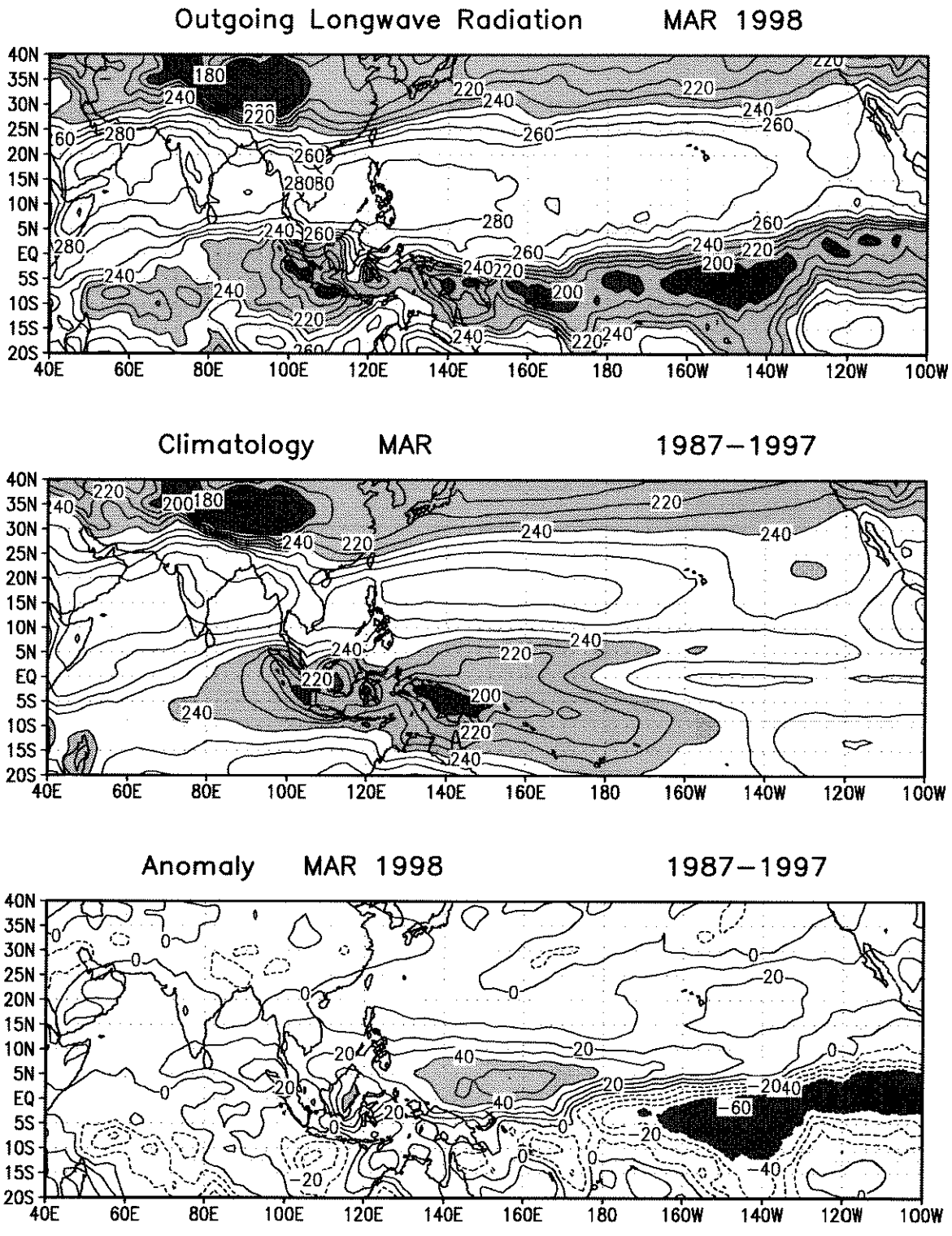

Figure 4b Same as Fig. 4a but for in March 1998.

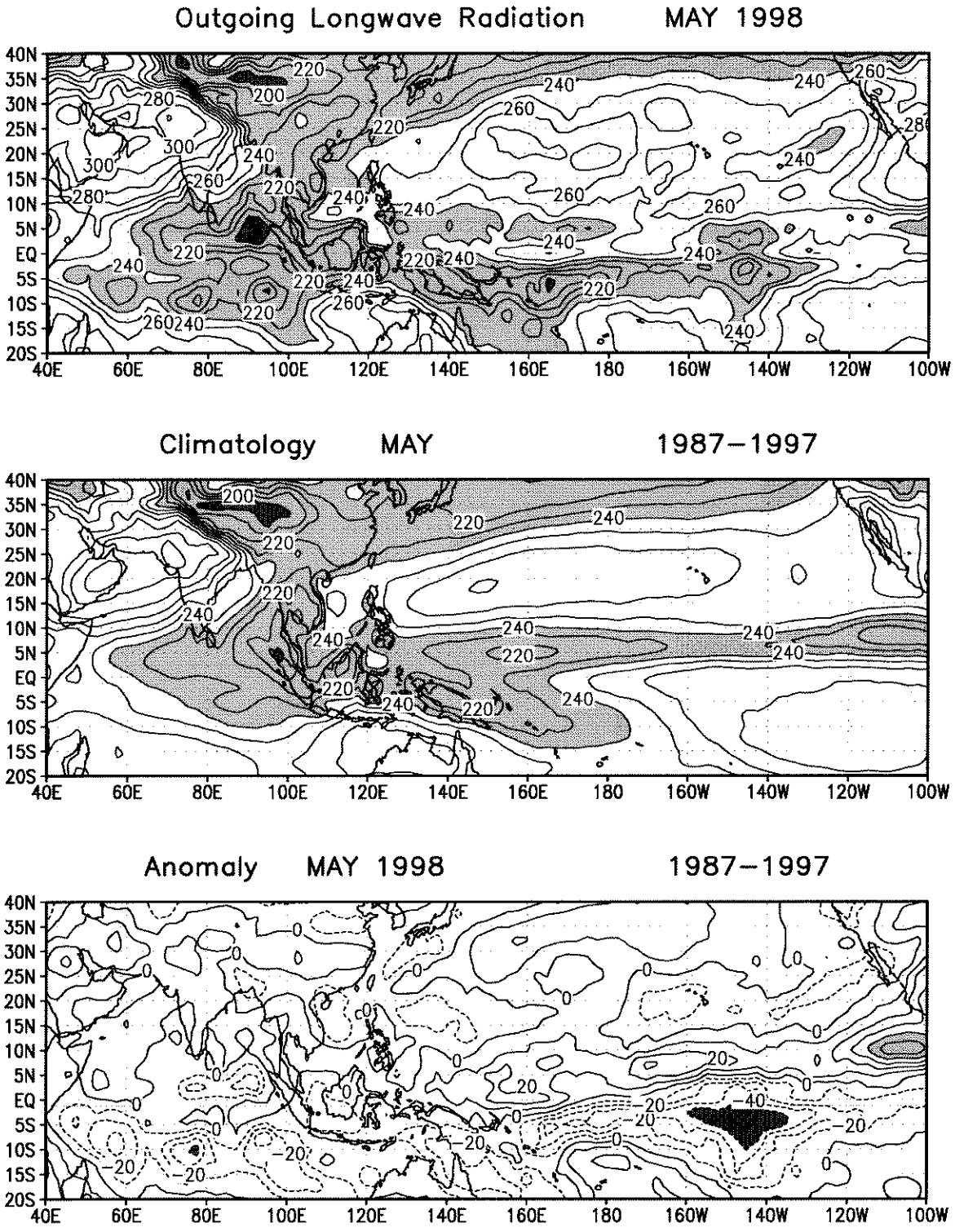

Figure 4c Same as Fig. 4a but for in May 1998.

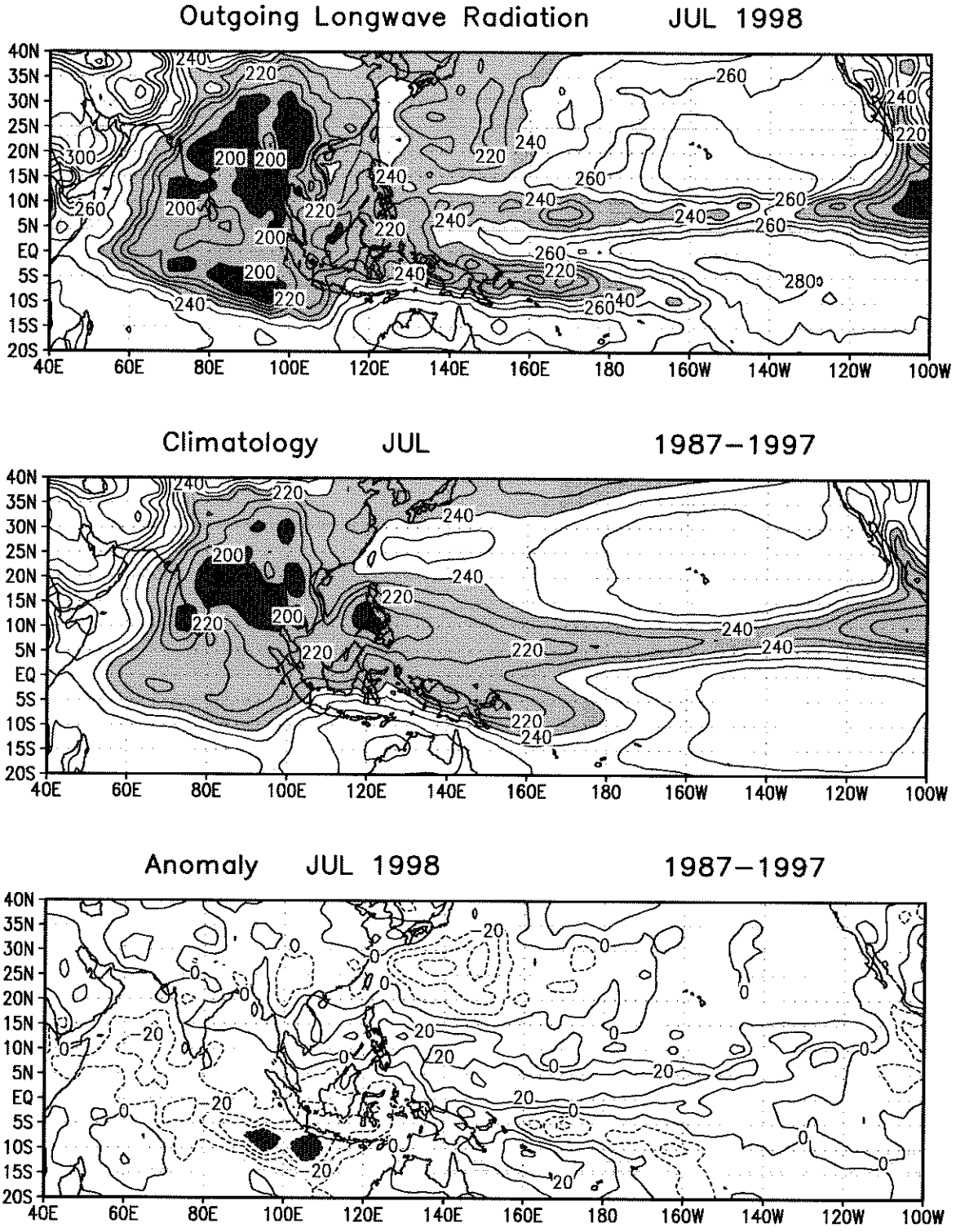

Figure 4d Same as Fig. 4a but for in July 1998.

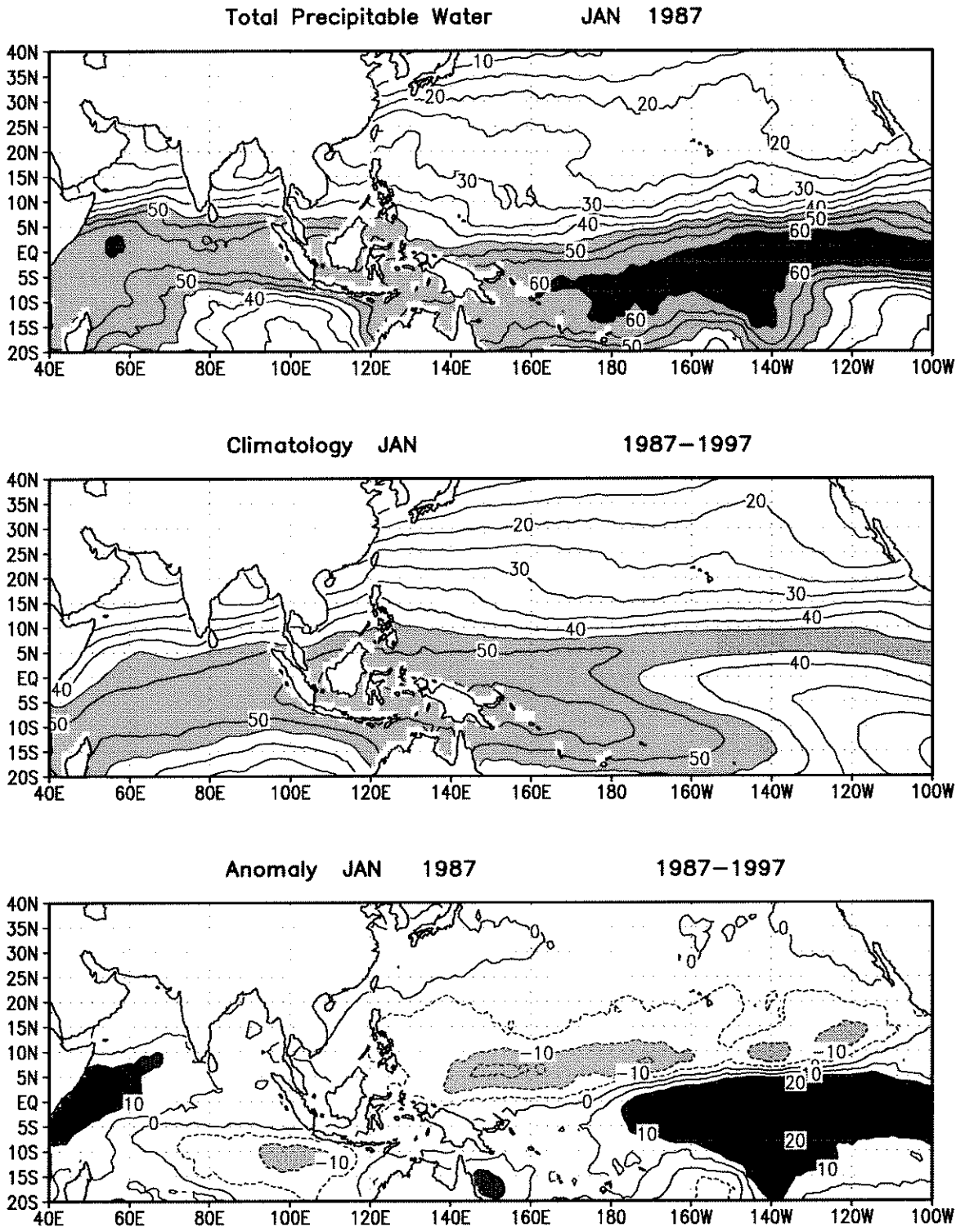

Figure 5a Same as in Fig. 3a but for the total precipitable water. Top: In January 1998. Heavy (light) shading denotes the region greater than 60(45) mm. Contour interval is 5 mm. Middle: Climatology. Shading and contour interval is the same as in the top figure. Bottom: Anomaly in January 1998. Heavy shading denotes the region greater than 10 mm , light shading less than -10 mm Contour interval is 5 mm.

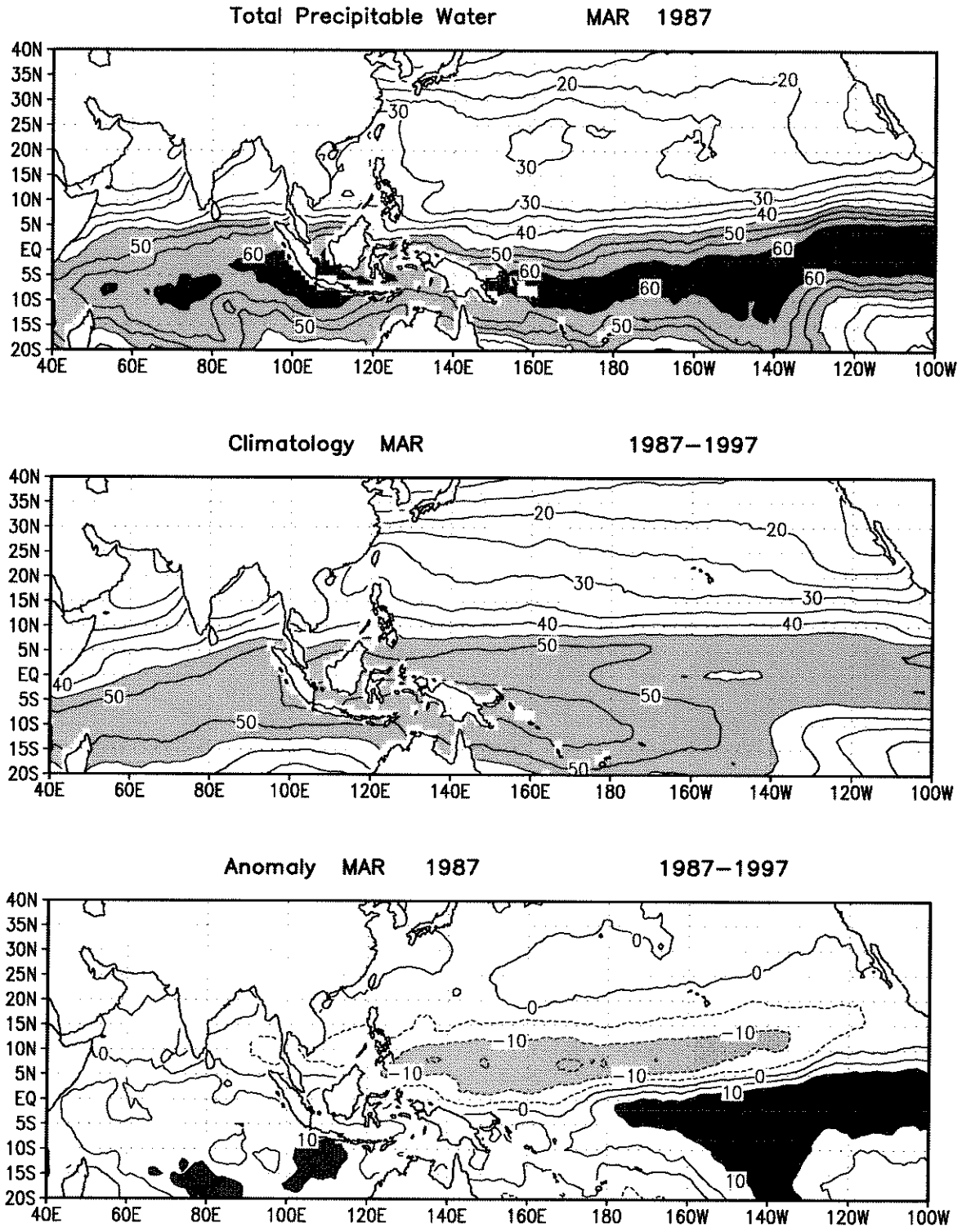

Figure 5b Same as Fig. 5a but for in March 1998.

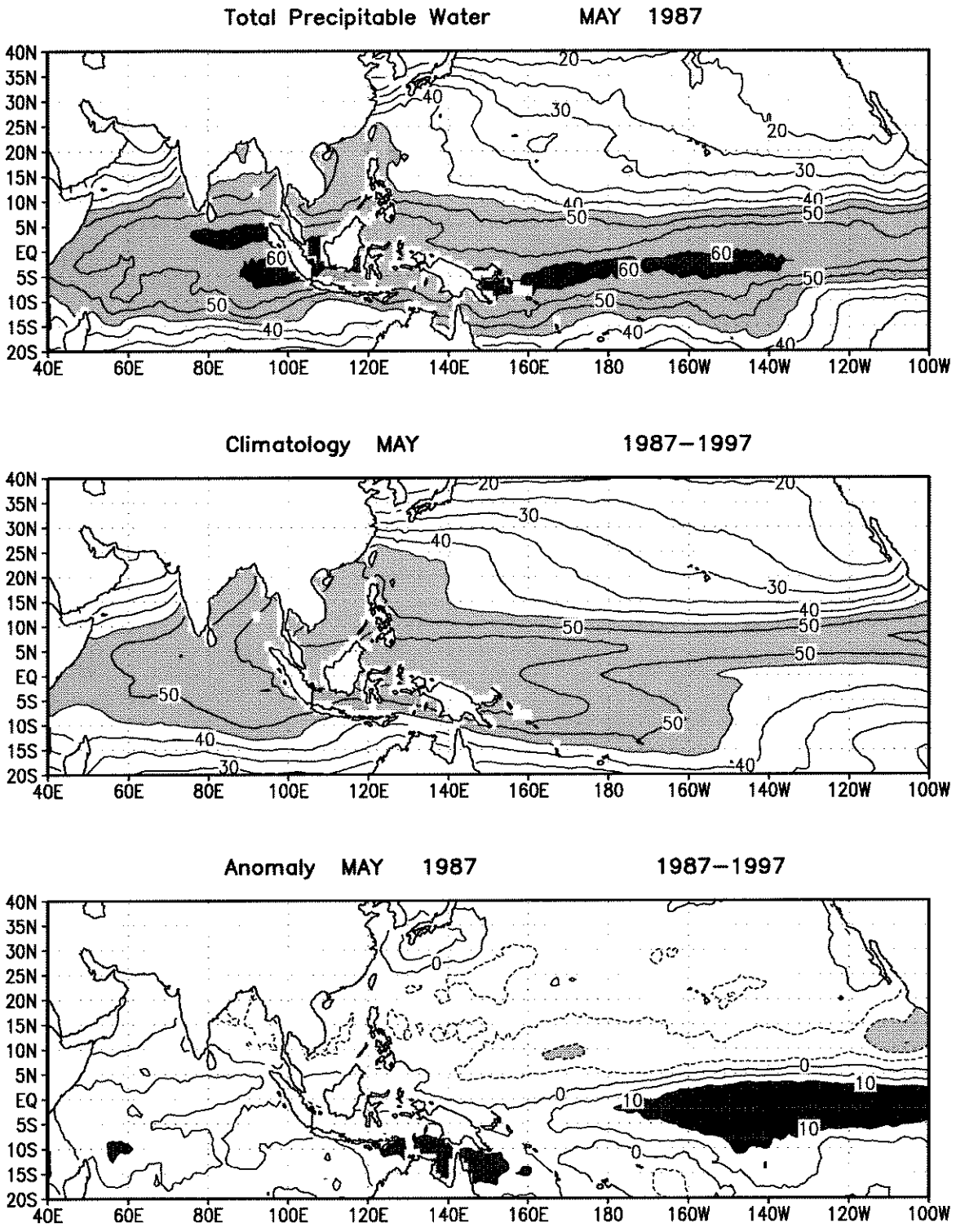

Figure 5c Same as Fig. 5a but for in May 1998.

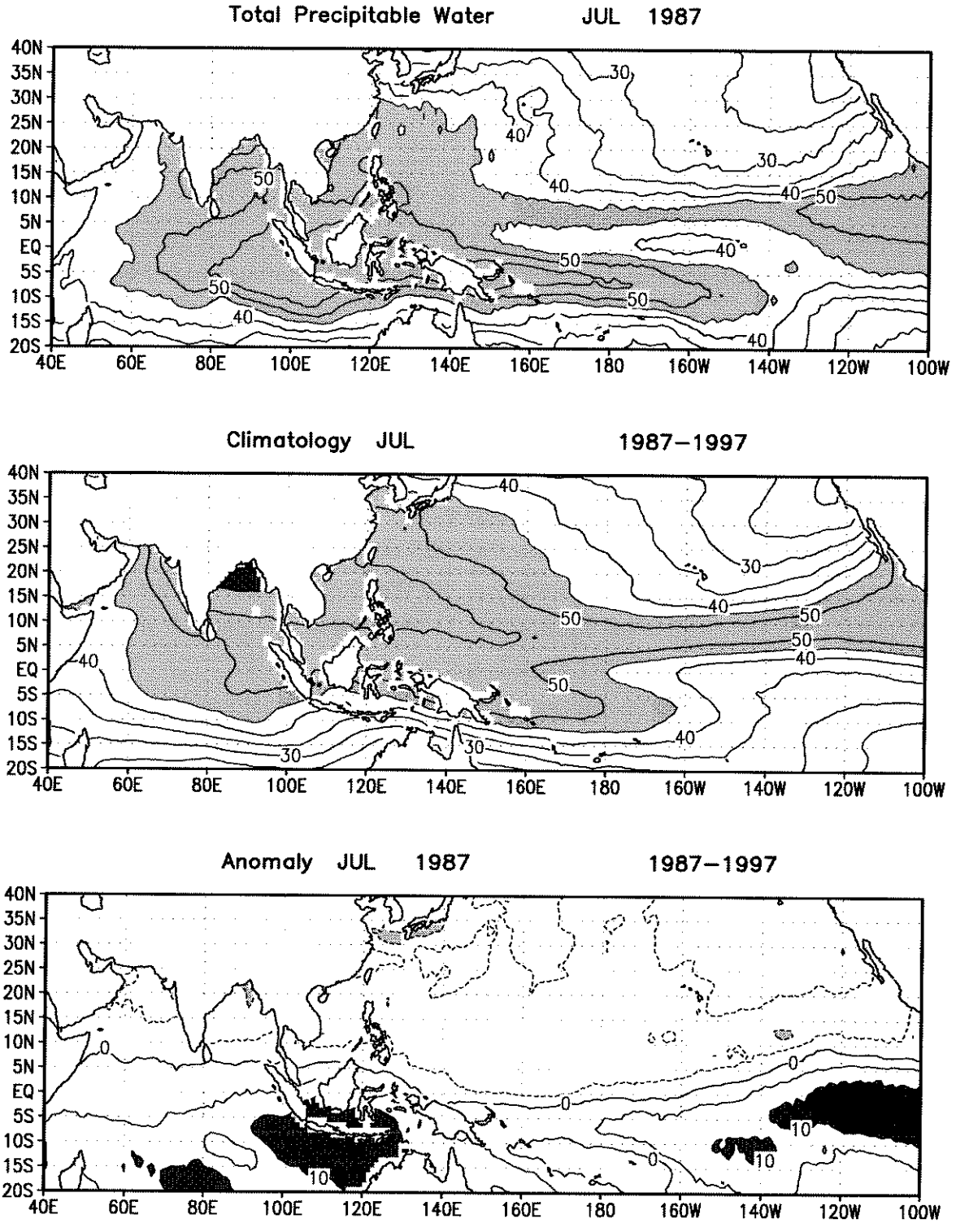

Figure 5d Same as Fig. 5a but for in July 1998.

although a reduced area of positive rainfall anomaly persists in this region (bottom panel). The July climatology for rainfall (middle panel) is maximum over the western Pacific in a generation region for tropical cyclones east of the Philippines. However, the monthly mean rainfall for July 1998 did not exceed 10 mm/day anywhere in this region. Similarly, a climatological maximum in rainfall occurs in the Bay of Bengal associated with the Indian summer monsoon. However, in July 1998 the monthly mean rainfall again did not exceed 10 mm/day in this region. Instead, the rainfall maximum in the Indian Ocean for July 1998 occurs in the Southern Hemisphere off Sumatra. The anomaly map (bottom panel) demonstrates these distinctions between hemispheres for rainfall anomaly across the Indian and Pacific Ocean basins; greater than normal rainfall in the Southern Hemisphere and lesser than normal rainfall in the Northern Hemisphere.

3b. Outgoing Longwave Radiation

Figure 4a-d depict the OLR which is a proxy for convective activity in the tropics. Lower OLR amplitudes indicate deeper convection, and negative anomalies in OLR indicate regions of more active convection. The patterns of OLR anomaly for all months (Fig. 4a-d) are in at least rough agreement with rainfall anomaly patterns just described (Fig. 3a-d).

In January 1998 a large negative anomaly (< -80 Wm^{-2}) region occupied the eastern Pacific (170 °W to 110 °W), just south of the equator (0 to 15 °S). Again, this anomaly is consistent with the mature phase of the 1997-98 ENSO warm event.

In contrast, in the western Pacific, an elongated east to west positive anomaly OLR signal spans 140 °E to 160 °E between the equator and 5 °N. This indicator of suppressed convection is in the position of the climatological ITCZ. This anomalous feature persisted until June 1998. However, by July 1998, after the relaxation of the ENSO warm event, the amplitude of the positive anomaly OLR in the western equatorial Pacific was reduced by half.

Nonetheless, weak positive anomaly OLR (reduced convective activity) spanned the equatorial Pacific and into the Northern Hemisphere; including the tropical cyclone generation region east of the Philippines. The 20 Wm^{-2} contour in Fig.4d (bottom) matches well with the negative anomaly rainfall in Fig.3d (bottom).

3c. Total Precipitable Water

Figure 5a-d show monthly mean TPW amounts from SSM/I. Again, the anomaly patterns by month are similar to those for surface wind speed, rainfall (Fig. 3), and OLR (Fig. 4). Regions of moist air anomalies in January 1998 include the western Indian Ocean off Africa and just south of the equator in the eastern Pacific. Regions of dry air anomalies in January 1998 are southwest of Sumatra and just north of the equator in the central and western Pacific. The moist air anomaly in the region just south of the equator in the eastern Pacific exceeds 60 mm (top panel, heavy shading).

This is in contrast to a climatological value that is less than 40 mm, creating an anomaly of more than 25 mm. The climatology is dry due to the regional oceanic upwelling that supplies colder water to the sea surface in normal years. Reduced ocean upwelling in this region is another

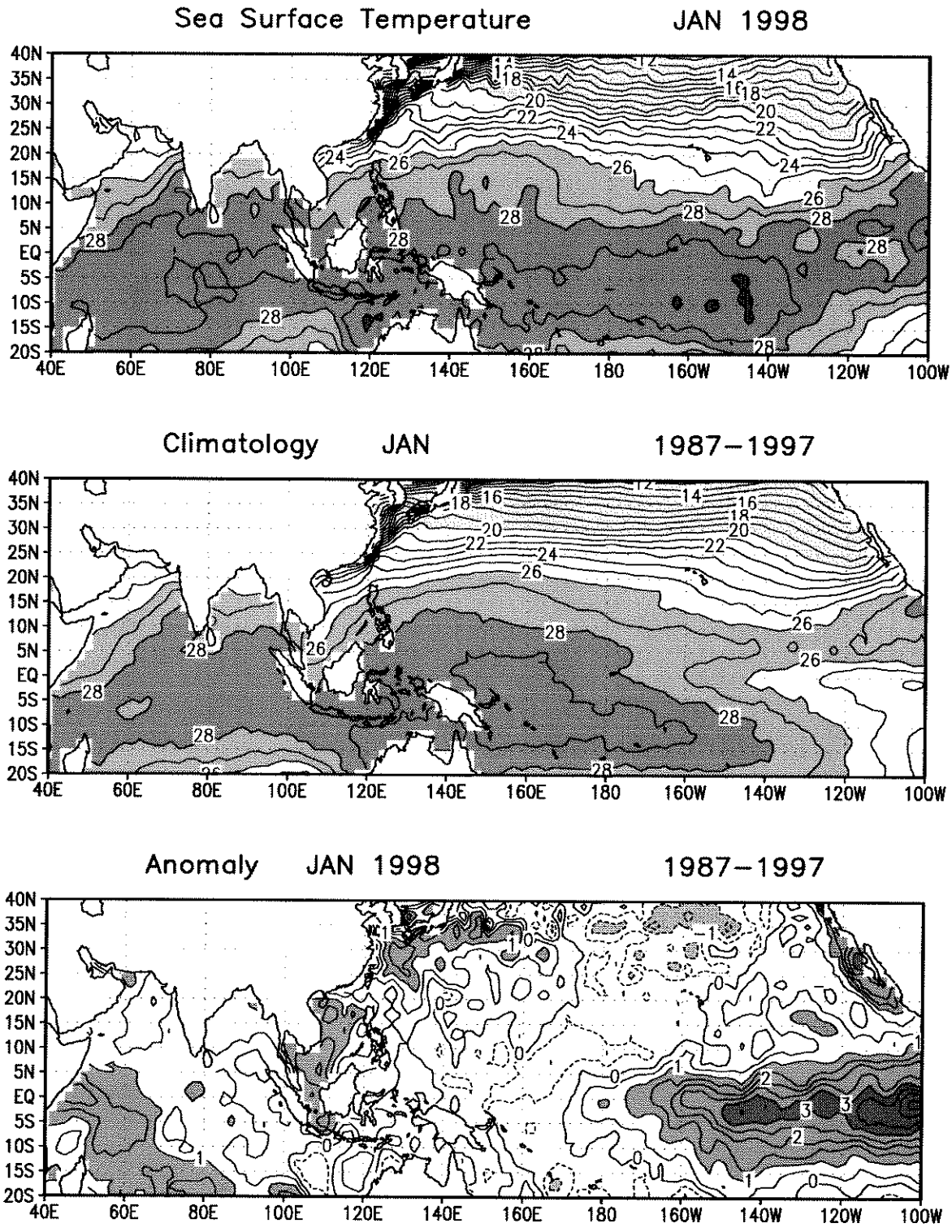

Figure 6a Same as in Fig. 3a but for the sea surface temperature(SST). Top: In January 1998. Heavy (light) shading denotes the region warmer than 28(26) °C. Contour interval is 1 °C. Middle: Climatology. Shading and contour interval is the same as in the top figure. Bottom: Anomaly in January 1998. Heavy(light) shading denotes the region warmer than 3(1) °C. Solid(dashed) contour line is for warm(cold) anomaly.

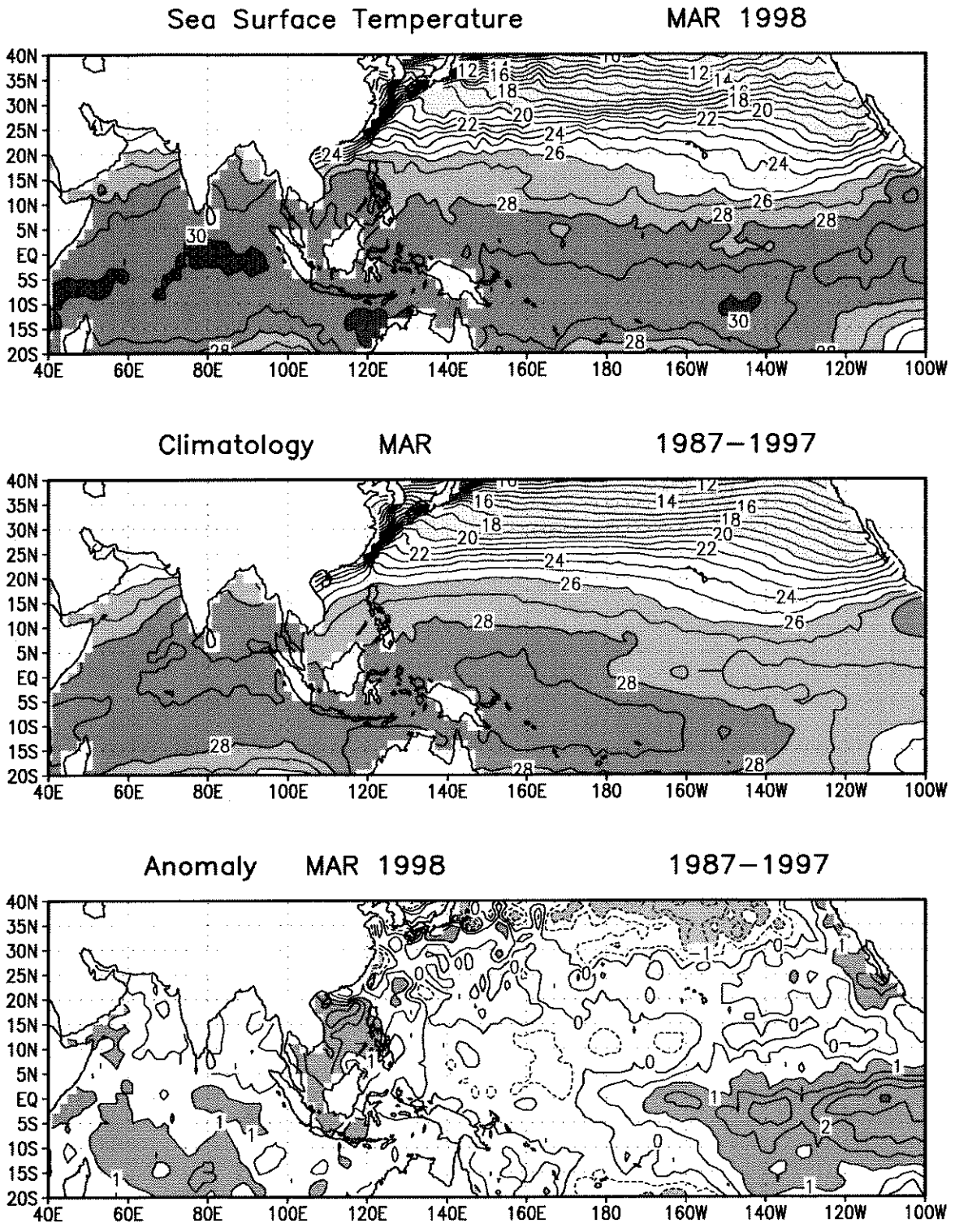

Figure 6b Same as Fig. 6a but for in March 1998.

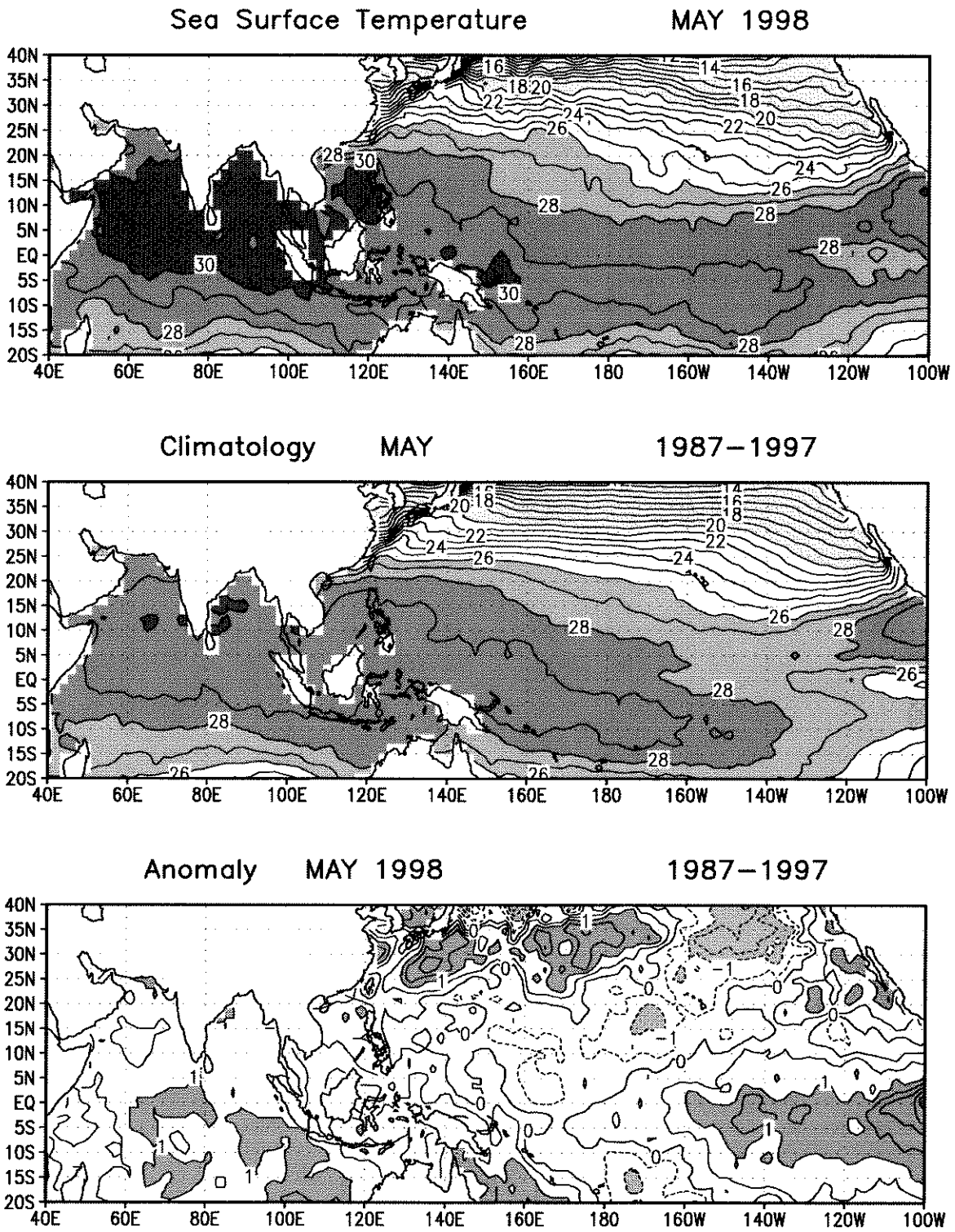

Figure 6c Same as Fig. 6a but for in May 1998.

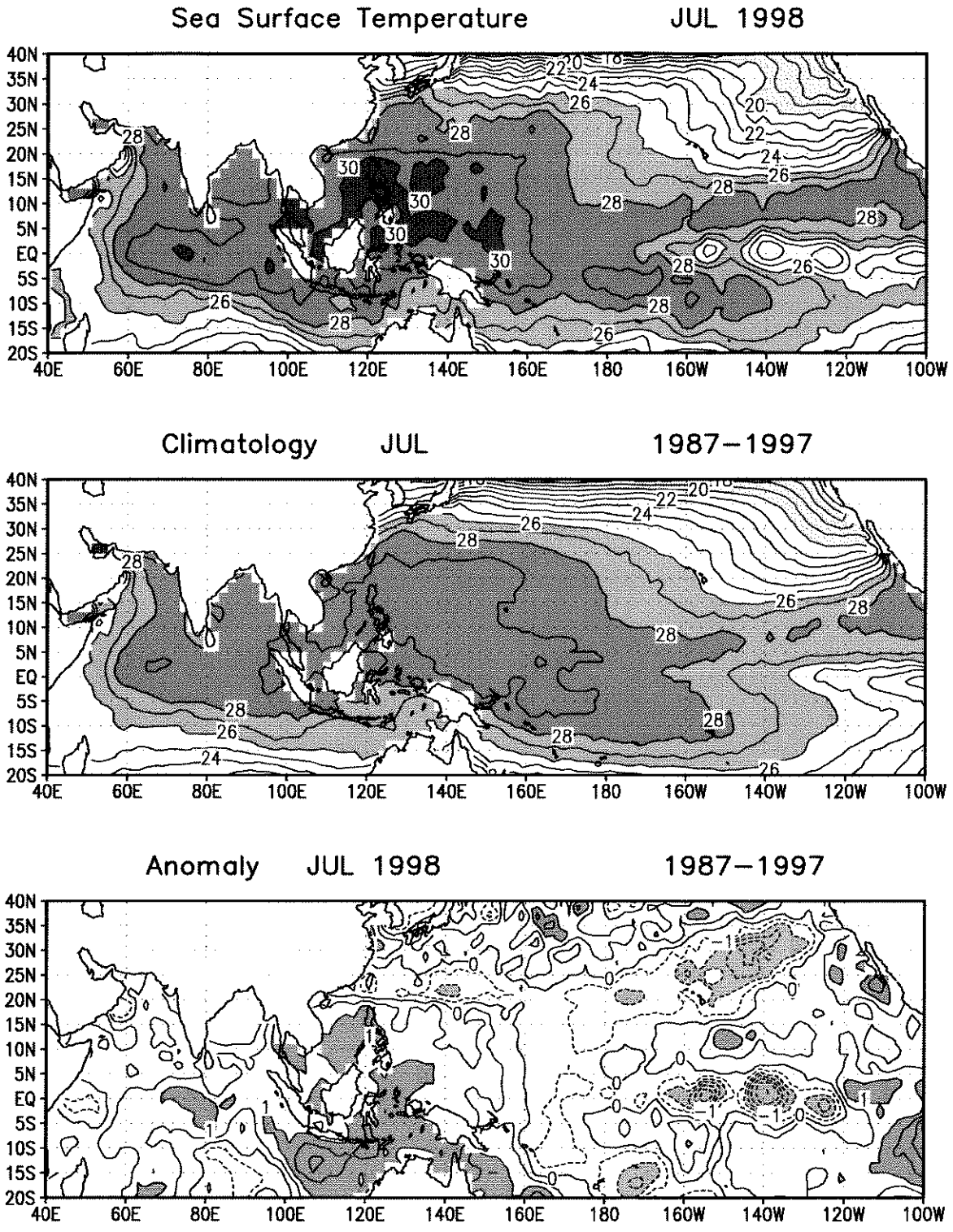

Figure 6d Same as Fig. 6a but for in July1998.

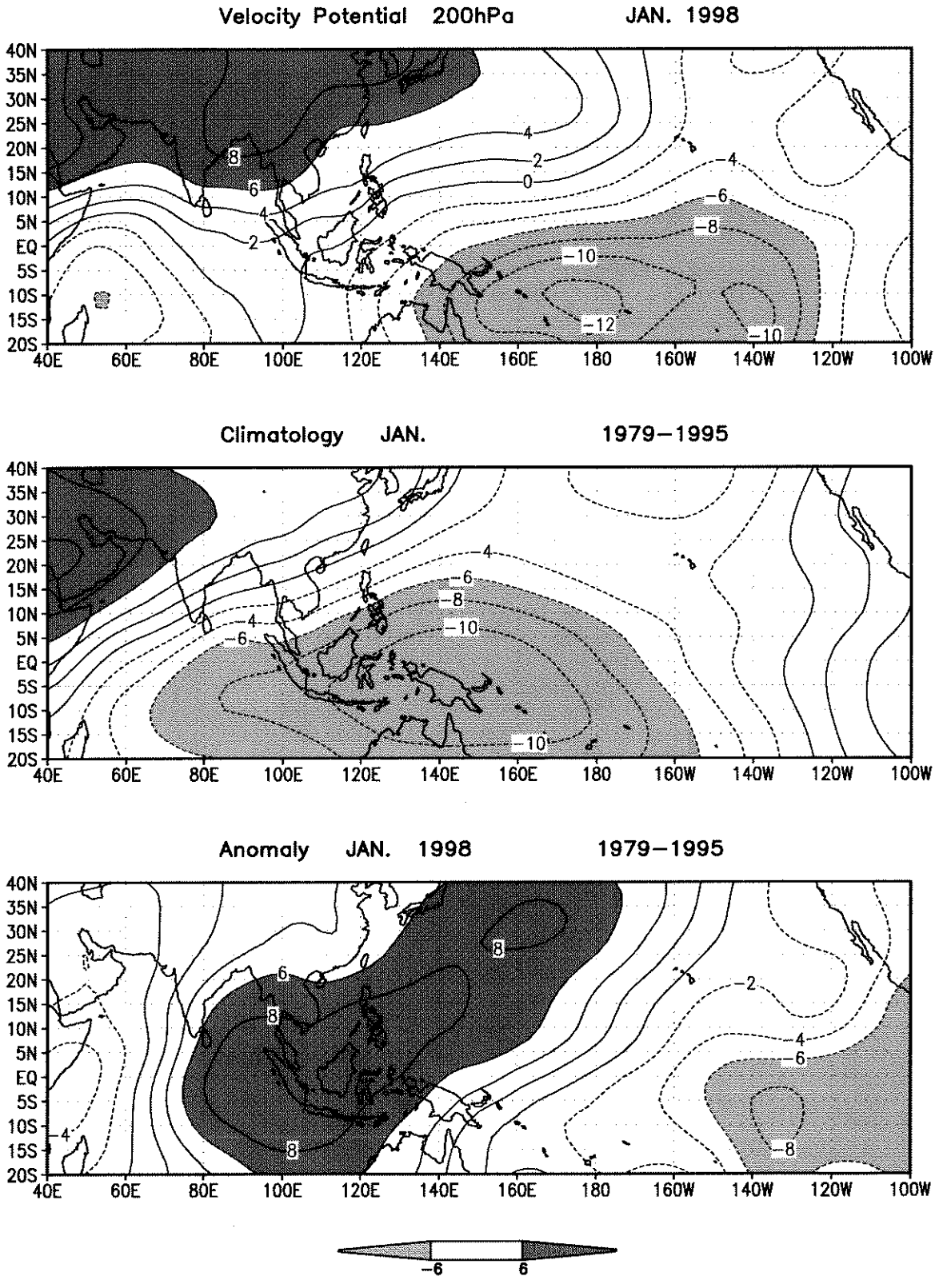

Figure 7a Same as in Fig. 3a but for the velocity potential at 200 hPa. Top: In January 1998. Middle: Climatology. Bottom: Anomaly in January 1998. Heavy (light) shading denotes the region greater(smaller) than +6(-6) x 10^6 sec^{-1}. Contour interval is 2 x 10^6 sec^{-1}.

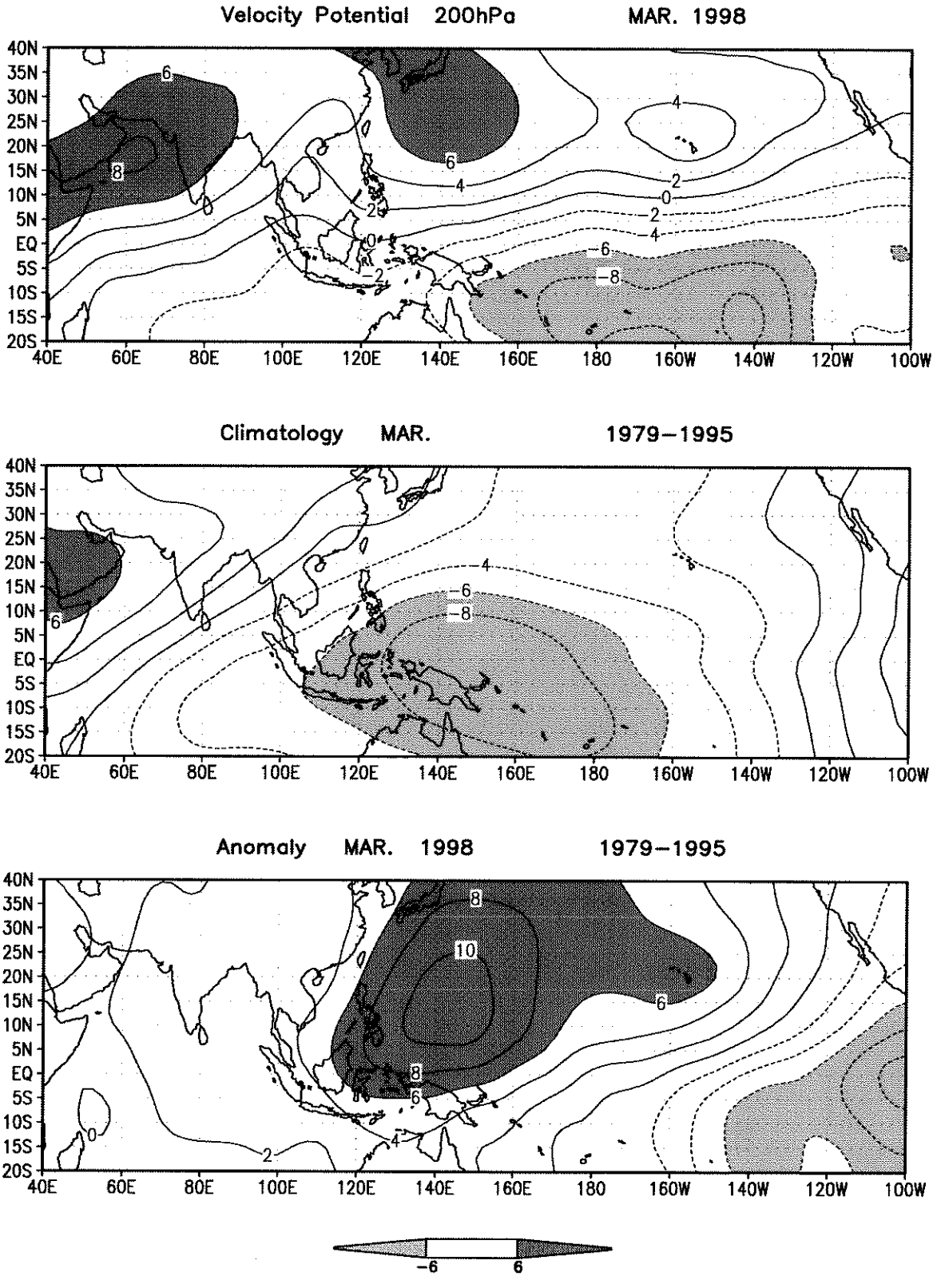

Figure 7b Same as Fig. 7a but for in March 1998.

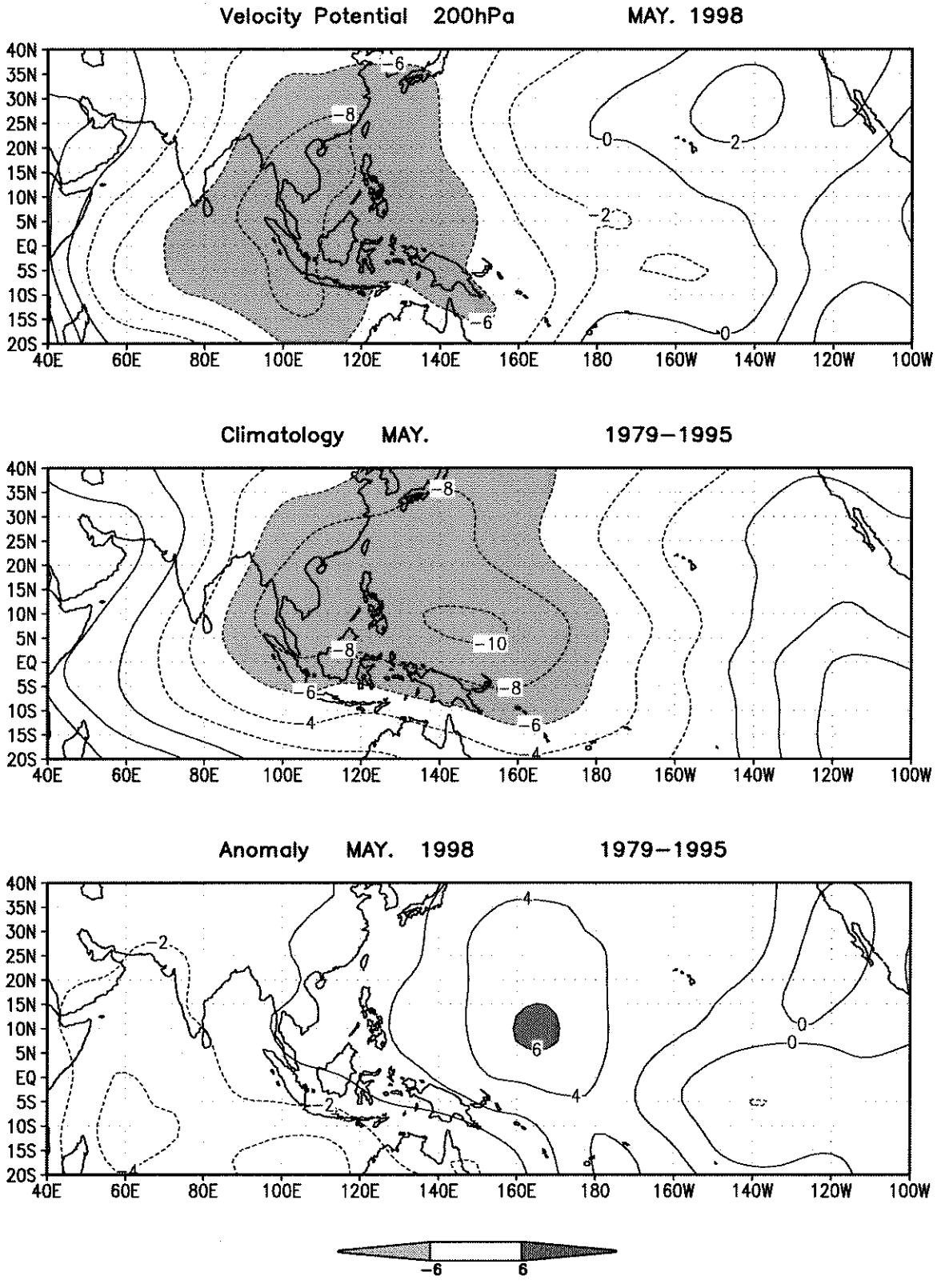

Figure 7c Same as Fig. 7a but for in May1998.

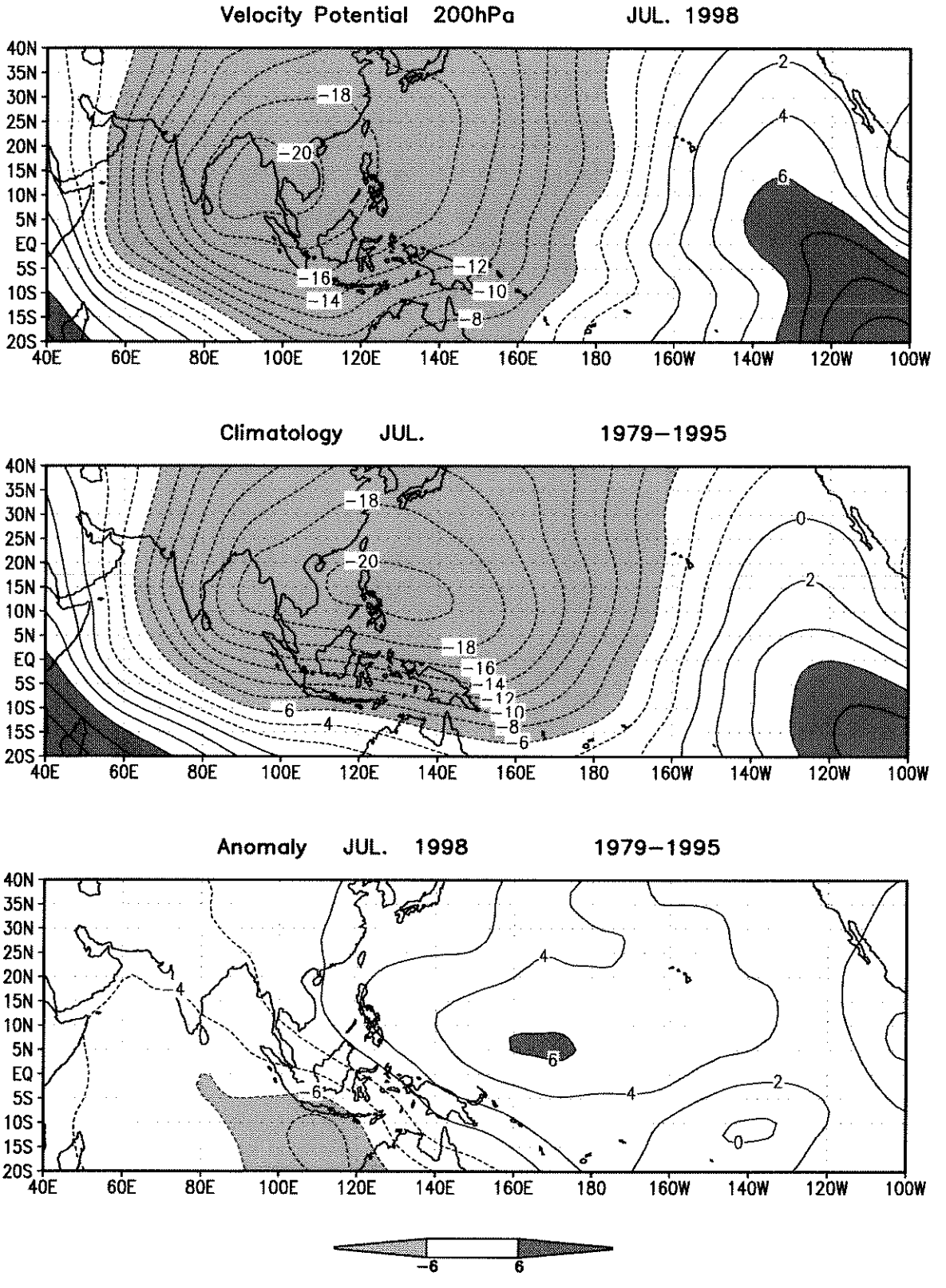

Figure 7d Same as Fig. 7a but for in July1998.

classical signal associated with ENSO warm events.

As for the patterns in 1998 rainfall (Fig 3b, c), the March (Fig 5b) and May (Fig 5c) patterns persisted in central location but diminished in area and/or amplitude.

By July 1998, the wetter than average air masses spanned the Southern Hemisphere tropics and sub-tropics (Fig 5d, bottom) while drier than average air characterized the Northern Hemisphere. This is unusual because July is the Southern Hemisphere winter and the climatology is for wetter air in the Northern Hemisphere (middle panel). Wet air anomalies greater than 15 mm occurred in the southeastern Indian Ocean (southwest of Sumatra) and in the eastern Pacific just south of the equator.

3d. Sea Surface Temperature

Perhaps the best known indicators of ENSO warm events have to do with SST. Figure 6 depicts the SST in the present study area and an anomalously high SST area (> 3 °C anomalies) appeared in the eastern Pacific in January 1998 (Fig 6a, bottom panel). The high SST anomaly in the eastern Pacific gradually abated through March and May.

By July 1998 a negative anomaly in SST appeared on the equator between 160 °W and 120 °W, possibly signalling the onset of an ENSO cold event (or La Niña) condition. A high SST anomaly (up to 1.5 °C) covers the southeastern Indian Ocean. The SST over the western Pacific was also higher than normal, exceeding 30 °C around the Philippines. This SST exceeds the threshold value for tropical cyclone formation attributed earlier to Palmén, but this condition does not appear to be sufficient by itself for cyclogenesis in 1998.

3e. Velocity Potential at 200 hPa

The velocity potential in the upper troposphere is shown in Figure 7a-d. For our study area, velocity potential values at 200 hPa that are less than zero denote upper-level divergence in the rising and outflow regions of atmospheric deep convection. Similarly, positive velocity potentials indicate convergence from which we infer subsiding air. Recall that we associated the suppressed tropical cyclone formation in 1998 with anomalous large-scale subsidence in the western Pacific.

Two centers of negative velocity potentials were located around 10 °S at the dateline and at 140 °W in the eastern tropical Pacific for January 1998 (Figure 7a, top panel). This contrasts with the climatological position for deep convection in January which locates over the Maritime Continent (Fig. 7a, middle panel). Thus the anomaly map for January 1998 (Fig 7a, bottom panel) suggests reduced convection or subsidence over the Maritime Continent fed by increased convection or rising motion just south of the equator in the eastern Pacific. The anomalous subsidence extends eastward into the western Pacific, in a region normally favored for tropical cyclogenesis. In fact, the January 1998 velocity potential map indicates no region in the western Pacific east of the Philippines with a value smaller than -6×10^6 sec^{-1}. This differs markedly from the climatology where normal conditions are favorable for cyclogenesis even in winter.

The 200 hPa velocity potential anomaly pattern is similar in March 1998, but the divergent region south of the equator in the eastern Pacific has weakened. The convergent region in the

western Pacific is shifted slightly eastward to 25 °N, 140 °E. Again, for climatological March, the divergent region is centered just east of the Maritime Continent, with significant divergence in the Northern Hemisphere western Pacific. As a result, the anomaly map for March 1998 is similar in pattern to January 1998, but the amplitude of the convergence (and therefore subsidence) in the western Pacific is stronger.

In the climatology, May marks the beginning of the Southeast Asian monsoon. The climatological upper-level divergence for May centers over the western Pacific. However, in May of 1998 the center is shifted westward over southeast Asia and extending into the southeastern Indian Ocean. The 200 hPa velocity potential anomaly map for May 1998 depicts suppressed convection over the western Pacific, and slightly enhanced convection in the Indian Ocean. The amplitudes of these anomalies are small compared with the anomalies for January and March 1998.

In July 1998, the upper-level divergence pattern strengthened over southeast Asia and the Bay of Bengal (less than -20 x 10^6 sec^{-1}). The westward shift persisted in the position of the velocity potential minimum with respect to the climatological position for July over the western Pacific, east of the Philippines. This difference in position for the minima (July 1998 vs. climatology) amounts to 30 ° in longitude. The 200 hPa velocity potential anomaly map for July 1998 is similar to the anomaly map for May 1998, but the anomalous divergence over the southeastern Indian Ocean has strengthened, suggesting that the Indian monsoon is slightly more active in 1998. The positive anomaly (convergence and subsidence) over the western Pacific has become more east-west oriented in the latitude band (5 to 10 °N) of the climatological ITCZ. Anomalous subsidence there is an effective suppressant for tropical cyclogenesis.

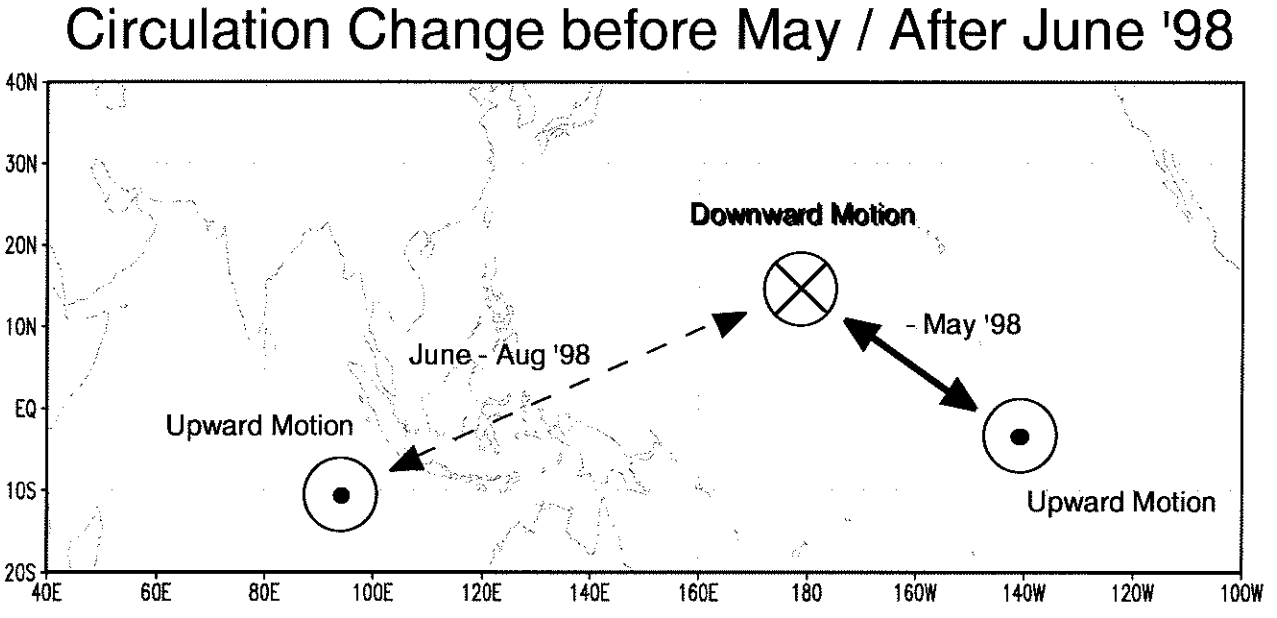

Figure 8 Schematic picture of the circulation change before May / after June 1998 over the Indian Ocean and the Pacific.

4. Conclusions

The recurring theme that emerges from these analyses is depicted in Figure 8. Prior to May 1998 the tropical Indian and Pacific ocean atmospheric circulation was dominated during the 1997-98 ENSO warm event. Rising motion dominated the region just south of the equator in the eastern Pacific, consistent with increased convection, greater TPW, and higher SST when compared to climatology. An anomalous center for compensating downward motion was located over the western Pacific where the air mass was anomalously dry in the climatological position of the ITCZ which was not present in early 1998. As we mentioned above, one mechanism for tropical cyclone formation (the coupling type) depends upon the presence of the climatological ITCZ.

In a climatological July, many tropical cyclones are generated in the western Pacific east of the Philippines. However, this region was the site of anomalous subsidence in July 1998 and tropical cyclone formation was suppressed. By July 1998, the source region for the subsidence in the western Pacific had shifted to the southeastern Indian Ocean. In this region the convection was anomalously active, the air mass was wetter than normal, and SST was higher. A higher SST anomaly over the western Pacific in July 1998 was not sufficient to generate tropical cyclones. This suggests the importance of other factors in tropical cyclogenesis. In this case we have examined thelarge-scale rising and subsiding motion, or local Walker circulation; as well as the moisture contents of the local air masses.

References

Aoki, T., 1985: A climatological study of typhoon formation and typhoon visit to Japan. Meteor. Geophys., 36, 61-118.

Gray, W. M., 1979: Hurricanes: their formation, structure and likely role in the tropical circulation. Meteorology Over the Tropical Oceans, D. B. Shaw, Ed., Roy. Meteor. Soc., 155-218.

Li, C., 1988: Actions of typhoon over the western Pacific (including the South China Sea) and El Niño. Adv. Atmos. Sci., 5, 107-115.

Nakazawa, T., 1986: Intraseasonal variations of OLR in the tropics during the FGGE year. J. Meteor. Soc. Japan, 64, 17-34.

Palmén, E., 1948: On the formation and structure of tropical hurricanes. Geophysica, 3, 26-38.

Takayabu, Y. N. and T. Nitta, 1993: 3-5 day-period disturbances coupled with convection over the tropical Pacific Ocean. J. Meteor. Soc. Japan, 71, 221-246.

Wentz, F., 1995: A well calibrated ocean algorithm for SSM/I. RSS Technical Report 101395.

Wentz, F., 1996: SSM/I rain retrievals within a unified all-weather ocean algorithm. RSS Technical Report 120196.

Wu, G. and N.-C. Lau, 1992: A GCM simulation of the relationship between tropical-storm formation and ENSO. Mon. Wea. Rev., 120, 958-976.